

The process $gg \rightarrow h_0 \rightarrow \gamma\gamma$ in the Lee-Wick Standard Model

F. KRAUSS*, T. E. J. UNDERWOOD^{†‡}, AND R. ZWICKY[§]

IPPP, Department of Physics, Durham University, Durham DH1 3LE, UK

Abstract:

The process $gg \rightarrow h_0 \rightarrow \gamma\gamma$ is studied in the Lee-Wick extension of the Standard Model (LWSM) proposed by Grinstein, O'Connell and Wise. In this model negative norm partners for each SM field are introduced with the aim to cancel quadratic divergences in the Higgs mass. All sectors of the model relevant to $gg \rightarrow h_0 \rightarrow \gamma\gamma$ are diagonalized and results are commented on from the perspective of both the Lee-Wick and higher derivative formalisms. Deviations from the SM rate for $gg \rightarrow h_0$ are found to be of the order of 15% – 5% for Lee-Wick masses in the range 500 GeV – 1000 GeV. Effects on the rate for $h_0 \rightarrow \gamma\gamma$ are smaller, of the order of 3% – 1% for Lee-Wick masses in the same range. These comparatively small changes may well provide a means of distinguishing the LWSM from other models such as universal extra dimensions where same-spin partners to Standard Model fields also appear. Corrections to determinations of CKM elements $|V_{t(b,s,d)}|$ are also considered and are shown to be positive, allowing the possibility of measuring a CKM element larger than unity, a characteristic signature of the ghost-like nature of the Lee-Wick fields.

*frank.krauss@durham.ac.uk

†t.e.j.underwood@durham.ac.uk

‡New address: *Max-Planck-Institut für Kernphysik, Saupfercheckweg 1, 69117 Heidelberg, Germany*

§roman.zwicky@durham.ac.uk

1 Introduction

The Higgs mechanism is one of the cornerstones of the Standard Model (SM) since it provides an elegant way of endowing the fundamental particles of the SM with mass. Therefore, it is not surprising that in past decades large efforts have been undertaken to find the Higgs boson and thus confirm this mechanism of electroweak symmetry breaking (EWSB). From a more theoretical point of view, the Higgs mechanism, however elegant, has a severe aesthetical flaw on the quantum level. Due to the emergence of quadratic divergences in the self-energy corrections of the scalar Higgs boson, there must be some essential fine-tuning in order for its physical mass to satisfy all constraints, including the upper limit of roughly 1 TeV stemming from unitarity requirements in $W_L W_L$ scattering. One viable method to significantly reduce the amount of fine-tuning consists of introducing new degrees of freedom such that the quadratic divergences disappear. To protect the disappearance, additional symmetries, like in the case of supersymmetry, have been postulated, or the mechanism of EWSB and the Higgs boson itself have been explained on different dynamical grounds like in the case of technicolour models, which render the Higgs boson a composite object. Furthermore, in the past years a number of models involving extra dimensions have been developed and discussed which aim to minimise the amount of fine tuning by reducing the upper scale of the theory.

On the basis of the work “Finite Theory of QED” by Lee and Wick (LW) [1, 2], Grinstein, O’Connell and Wise (GOW) [3] proposed an extension of the SM which is free from quadratic divergences¹. The basic idea of Lee and Wick was to assume that the regulator employed in the framework of Pauli-Villars regularisation indeed is a physical degree of freedom which is not removed from the amplitudes. The scale of the LW masses has to be high enough to evade current experimental constraints and low enough in order to solve the hierarchy problem. Moreover, in the context of the see-saw mechanism for neutrino masses, it was shown in Ref. [4] that the presence of a very heavy right handed neutrino does not introduce destabilizing corrections to the Higgs mass of the form $\delta m_H^2 \sim m_{\nu_R}^2$, provided that $m_{\nu_R} \gg m_{\nu_L}$. This is unlike the minimal see-saw extension of the SM, where destabilizing corrections of the type mentioned above do appear.

However, a number of questions emerge concerning the interpretation and consequences of the Pauli-Villars “wrong-sign” states. A formal argument in favour of unitarity was given in Refs. [2, 5], based on the idea that once interactions are switched on, the negative norm states mix with physical multiparticle states into states with complex masses. The orthogonality of those states with the physical states then ensures that the S-matrix does map one type into the other. This is a necessary condition for the unitarity of the S-matrix restricted to the physical (positive norm) subspace. An illustrative example of how the finite width preserves unitarity can be found in [3, 6]. Contrary to the regular finite width, the complex masses are situated on the physical sheet upsetting the usual analytic structure. This demands a modification to the integration contour in the complex plane in order to eliminate exponentially growing modes [2, 7]. Consistent

¹ However, it is worth emphasizing that the Lee-Wick SM is not finite, contrary to LW QED [3].

results using this approach were obtained order-by-order in perturbation theory in Refs. [5, 6].

This modification of the integration contour leads to acausal effects [2, 5, 6] on the time scale of the inverse width of the LW state. The width Γ_{LW} of the LW resonances under consideration is too large for the time scales which can be resolved at current colliders. On the other hand, in this paper, finite width effects will be neglected since the LW mass scales and the difference between the LW and SM masses are much larger than the LW width, $m_{\text{LW}} \gg \Gamma_{\text{LW}}$ and $(m_{\text{LW}} - m_{\text{SM}}) \gg \Gamma_{\text{LW}}$.

A non-perturbative definition of the Lee-Wick approach using path integrals was first investigated in Ref. [8] but, as the authors state, the relation to the LW prescription remained unclear. The Euclidian path integral in the Higgs sector was then studied almost ten years later [9, 10], with the aim of investigating the triviality bound on the Higgs mass from the lattice using a symmetry preserving regularization. There it was clearly stated that the ghost poles due not allow a continuation to Minkowski space. Recently a path integral formulation has been advocated based on a test function space [11], which allows the continuation to a convergent Minkowski space formulation. Moreover, in that work the Lee-Wick contour prescription was derived from a path integral approach. It is worth mentioning that this prescription does not correspond to adding convergence factors to the action and therefore clarifies why earlier attempts were not able to relate the Euclidian path integral and the LW formulation.

In their recent paper, GOW made use of the fact that regularising Pauli-Villars-like states may be obtained from higher derivative terms in the Lagrangian. To illustrate this and to show how the additional fields of the LW approach cancel the quadratic divergences in the LW model, a toy model will be considered, similar to the one proposed by GOW [3], of a self-interacting, real scalar field $\hat{\phi}$, with a higher derivative term in the Lagrangian density

$$\mathcal{L}_{\text{hd}} = \frac{1}{2}(\partial_\mu \hat{\phi})(\partial^\mu \hat{\phi}) - \frac{1}{2}m^2 \hat{\phi}^2 - \frac{1}{2M^2}(\partial^2 \hat{\phi})^2 - \frac{\lambda}{4!} \hat{\phi}^4. \quad (1)$$

Taken directly from this Lagrangian, the propagator of the $\hat{\phi}$ field reads

$$\hat{D}(p) = \frac{i}{p^2 - p^4/M^2 - m^2} = \frac{-iM^2}{(p^2 - m_{\text{phys}}^2)(p^2 - M_{\text{phys}}^2)}, \quad (2)$$

in momentum space, where

$$m_{\text{phys}}^2[M_{\text{phys}}^2] = \frac{1}{2} \left(M^2 - [+] \sqrt{M^4 - 4m^2 M^2} \right), \quad (3)$$

are the physical masses. A possible interpretation is that, effectively, this theory describes two degrees of freedom with masses m_{phys} and M_{phys} , respectively. The authors of [3] have shown how to make these degrees of freedom manifest by introducing an auxiliary “Lee-Wick” field $\tilde{\phi}$ of mass M , such that the Lagrangian becomes

$$\mathcal{L}_{\text{aux}} = \frac{1}{2}(\partial_\mu \hat{\phi})(\partial^\mu \hat{\phi}) - \frac{1}{2}m^2 \hat{\phi}^2 - \tilde{\phi} \partial^2 \hat{\phi} + \frac{1}{2}M^2 \tilde{\phi}^2 - \frac{\lambda}{4!} \hat{\phi}^4. \quad (4)$$

The higher derivative Lagrangian Eq. (1) may be recovered from Eq. (4) by employing the equation of motion (EoM) $M^2\tilde{\phi} = \partial^2\hat{\phi}$. Furthermore, by decomposing the field of the higher-derivative theory $\hat{\phi}$ into a “standard” field ϕ and a LW field $\tilde{\phi}$, through the shift $\hat{\phi} = \phi - \tilde{\phi}$, the Lagrangian can be written

$$\mathcal{L}_{\text{eff}} = \frac{1}{2}(\partial_\mu\phi)(\partial^\mu\phi) - \frac{1}{2}(\partial_\mu\tilde{\phi})(\partial^\mu\tilde{\phi}) - \frac{1}{2}m^2(\phi - \tilde{\phi})^2 + \frac{1}{2}M^2\tilde{\phi}^2 - \frac{\lambda}{4!}(\phi - \tilde{\phi})^4. \quad (5)$$

Clearly, in the presence of m , the two states ϕ and $\tilde{\phi}$ mix. The Lagrangian can be expressed in terms of mass eigenstates after a symplectic transformation on the fields

$$\begin{pmatrix} \phi \\ \tilde{\phi} \end{pmatrix} = \begin{pmatrix} \cosh\theta & \sinh\theta \\ \sinh\theta & \cosh\theta \end{pmatrix} \begin{pmatrix} \phi' \\ \tilde{\phi}' \end{pmatrix}, \quad \tanh 2\theta = \frac{-2m^2/M^2}{1 - 2m^2/M^2}, \quad (6)$$

where the constraint, $2m < M$ must be satisfied, leading to the constraint on the physical masses $m_{\text{phys}} < M_{\text{phys}}$. Expressed in the new basis, the Lagrangian density becomes

$$\mathcal{L}_{\text{eff}} = \frac{1}{2}(\partial_\mu\phi')(\partial^\mu\phi') - \frac{1}{2}(\partial_\mu\tilde{\phi}')(\partial^\mu\tilde{\phi}') - \frac{1}{2}m_{\text{phys}}^2\phi'^2 + \frac{1}{2}M_{\text{phys}}^2\tilde{\phi}'^2 - \frac{\lambda_{\text{phys}}}{4!}(\phi - \tilde{\phi})^4. \quad (7)$$

The ultraviolet behaviour of this theory can be accessed from the Lagrangian of Eq. (7), where from now on the primes are dropped. At order $\mathcal{O}(\lambda)$, for instance, the self-energy correction to the ϕ field has two tadpole contributions, where either ϕ or $\tilde{\phi}$ run in the loop. Employing dimensional regularisation with $d = 4 - 2\varepsilon$, they read

$$\Sigma(p^2) = i\lambda \left(\int \frac{d^d k}{(2\pi)^d} \frac{i}{k^2 - m^2} - \int \frac{d^d k}{(2\pi)^d} \frac{i}{k^2 - M^2} \right) = i\lambda \int \frac{d^d k}{(2\pi)^d} \frac{i(m^2 - M^2)}{(k^2 - m^2)(k^2 - M^2)},$$

and apparently the quadratic divergence has been reduced to a logarithmic one. This is the anticipated result, since the introduction of higher-derivative terms in the way proposed by GOW leads to higher powers of the momentum in the propagators of the full theory, thus improving the convergence of graphs. Effects of higher derivative terms in the interactions could eventually upset this picture, however such terms are not present in the toy model discussed here. For the full LW version of the SM, studied in Sec. 2, the situation is not so clear.

In the past few months various consequences of the LW extension of the SM (LWSM) have been discussed, in particular the prospects for finding LW bosons at the LHC [12] and LW effects in flavour physics [13]. This publication aims at a first study of the phenomenology of the LWSM at loop level in the “golden-plated” discovery modes for low-mass Higgs bosons at the LHC, $gg \rightarrow h_0 \rightarrow \gamma\gamma$. Following the reasoning above, one would naively expect similarly strong cancellations in all kinds of loop-induced processes, effectively suppressing a plethora of interesting signals, such as, e.g. $gg \rightarrow h_0 \rightarrow \gamma\gamma$.

So the outline of this paper is as follows; in section 2 the initial work of GOW on the construction of the LWSM will be supplemented with a discussion of all transformations from the original degrees of freedom into the mass eigenstates. Then the exact cancellation of quadratic divergences in the Higgs self-energy will be checked. In section 4, the decay

widths for $h_0 \rightarrow gg$ and $h_0 \rightarrow \gamma\gamma$ will be calculated in the LWSM. They will be multiplied such that the overall cross section for $gg \rightarrow h_0 \rightarrow \gamma\gamma$ can be obtained and compared to results from other models, such as universal extra dimensions (UEDs). Furthermore, in this section, some of the phenomenological consequences will be highlighted. Section 5 will outline some interesting effects in the flavour physics sector, in particular related to the determination of CKM matrix elements. Some short discussion of potential further effects of this model and how it can be distinguished from other models beyond the Standard Model round off the publication, before its central findings are summarised.

2 The Lagrangian of the Lee-Wick Standard Model

2.1 Construction principle

The principle idea underlying the Lee-Wick extension of the SM constructed by GOW is to augment the SM Lagrangian with higher derivative terms. Of course, in principle a huge number of such terms are allowed, see for instance [14, 15], but only few of them are actually selected for the construction of the LWSM. In particular;

- for each scalar, a term

$$- \frac{1}{M_\phi^2} (\hat{D}_\mu \hat{D}^\mu \hat{\phi})^\dagger (\hat{D}_\nu \hat{D}^\nu \hat{\phi}) \quad (8)$$

is introduced (see also the toy model in the introduction), where D^μ is the gauge covariant derivative;

- for each fermion, a term

$$+ \frac{1}{M_\psi^2} \bar{\hat{\psi}} i \hat{\not{D}} \hat{\not{D}} \hat{\not{D}} \hat{\psi} \quad (9)$$

is added;

- and for each gauge field, a term

$$+ \frac{1}{M_A^2} \text{Tr}(\hat{D}^\mu \hat{F}_{\mu\nu}) (\hat{D}^\lambda \hat{F}_\lambda{}^\nu) \quad (10)$$

is added. The field strength tensor is generalised to

$$\hat{F}^{\mu\nu} = \partial_\mu \hat{A}_\nu - \partial_\nu \hat{A}_\mu - ig[\hat{A}_\mu, \hat{A}_\nu] \quad \text{with} \quad \hat{A}_\mu = \hat{A}_\mu^A T^A, \quad (11)$$

where T^A are the generators of the corresponding gauge group with coupling constant g .

It should be stressed that the rest of the structure of the SM, in particular the interactions, remains unchanged apart from replacing the original SM fields with the “hatted” fields of the higher derivative theory.

2.2 Higgs sector

In the Higgs sector of the LWSM, higher derivative terms of the form of Eq. (8) are eliminated in a way identical to the toy model; auxiliary fields \tilde{H} are introduced and their EoM are used to replace the higher derivative terms with mass terms and kinetic terms for the auxiliary fields. The kinetic terms between \hat{H} and \tilde{H} are diagonalized by applying a shift $\hat{H} = H - \tilde{H}$. Further diagonalization of the Higgs mass matrix proceeds in the same fashion as in the toy model studied by GOW and in the introduction. Thus, in the unitary gauge the two doublets are

$$H^\top = [0, (v + h_0)/\sqrt{2}] , \quad \tilde{H}^\top = [\tilde{h}_+, (\tilde{h}_0 + i\tilde{P}_0)/\sqrt{2}] , \quad (12)$$

where h_0 refers to the SM-like neutral Higgs boson, \tilde{h}_+ , \tilde{h}_0 , and \tilde{P}_0 refer to the charged and neutral scalar and pseudoscalar LW Higgs bosons, respectively. Apart from their negative norm, this added Higgs-doublet is a structure which can be found in many extensions of the SM, most prominently in the MSSM. It is worth stressing at this point that the LW Higgs doublet \tilde{H} does not acquire a vacuum expectation value.

2.2.1 Neutral, CP-even Higgs bosons

The kinetic term for the neutral, CP-even Higgs bosons reads

$$\mathcal{L}_h = \frac{1}{2} \left(\hat{D}_\mu \mathcal{H} \right)^\dagger \eta_2 \left(\hat{D}^\mu \mathcal{H} \right) - \frac{1}{2} \mathcal{H}^\dagger \mathcal{M}_h \eta_2 \mathcal{H} , \quad (13)$$

where the covariant derivative \hat{D}_μ is defined as

$$\hat{D}_\mu = \partial_\mu + i(\mathbf{A}_\mu + \tilde{\mathbf{A}}_\mu) , \quad (14)$$

with the abbreviation $\mathbf{A}_\mu = gA_\mu^a T^a + g_2 W_\mu^a T^a + g_1 B_\mu Y$ for all SM gauge fields and $\tilde{\mathbf{A}}_\mu$ the analogous expression for the LW versions of the gauge fields. Furthermore, the two CP-even scalars of the theory, h_0 and \tilde{h}_0 are now arranged in a vector \mathcal{H} , and they mix

$$\mathcal{H} = \begin{pmatrix} h_0 \\ \tilde{h}_0 \end{pmatrix} , \quad \mathcal{M}_h \eta_2 = \frac{1}{2} \begin{pmatrix} \lambda v^2 & -\lambda v^2 \\ -\lambda v^2 & \lambda v^2 - 2M_H^2 \end{pmatrix} \quad \text{and} \quad \eta_2 = \begin{pmatrix} 1 & 0 \\ 0 & -1 \end{pmatrix} . \quad (15)$$

The matrix $\mathcal{M}_h \eta_2$ can only be diagonalized if $M_H > \sqrt{2\lambda} v$. The diagonalization is achieved by the symplectic transformation S_h satisfying

$$S_h = \begin{pmatrix} \cosh \phi_h & \sinh \phi_h \\ \sinh \phi_h & \cosh \phi_h \end{pmatrix} , \quad S_h \eta_2 S_h^\dagger = \eta_2 , \quad (16)$$

where the fields \mathcal{H} and the matrix \mathcal{M}_h transform as

$$\mathcal{H}_{\text{phys}} = \eta_2 S_h^\dagger \eta_2 \mathcal{H} , \quad \mathcal{M}_{h,\text{phys}} \eta_2 = S_h^\dagger \mathcal{M}_h \eta_2 S_h . \quad (17)$$

For the sake of notational brevity the suffix “phys” will be dropped later on for the fields but it will be retained on the matrices and the mass eigenvalues for clarity. The symplectic rotation angle ϕ_h and the diagonalized mass matrix $\mathcal{M}_{h,\text{phys}}$ are given by

$$\tanh 2\phi_h = \frac{-\lambda v^2/M_H^2}{1 - \lambda v^2/M_H^2}, \quad (18)$$

and

$$\mathcal{M}_{h,\text{phys}} = \begin{pmatrix} \frac{1}{2} \left(M_H^2 - \sqrt{M_H^4 - 2v^2\lambda M_H^2} \right) & 0 \\ 0 & \frac{1}{2} \left(M_H^2 + \sqrt{M_H^4 - 2v^2\lambda M_H^2} \right) \end{pmatrix}, \quad (19)$$

where the physical masses are the same as in the toy model Eq. (3) with appropriate substitutions. In terms of the physical neutral Higgs boson masses $m_{h_0,\text{phys}}$ and $m_{\tilde{h}_0,\text{phys}}$ the quartic coupling λ can simply be written

$$\lambda v^2 = \frac{2m_{h_0,\text{phys}}^2 m_{\tilde{h}_0,\text{phys}}^2}{m_{h_0,\text{phys}}^2 + m_{\tilde{h}_0,\text{phys}}^2}. \quad (20)$$

Prior to diagonalization of the neutral Higgs boson mass matrix, from Eq. (13) notice that the LW Higgs fields do not couple to gauge bosons via a trilinear coupling after electroweak symmetry breaking, suggesting a “gaugeophobic” structure. This follows from the fact that the \tilde{H} does not acquire a VEV. However, after diagonalization, mixing will induce these trilinear couplings with a strength proportional to the hierarchy between the SM-like and LW Higgs masses.

2.3 Fermions

2.3.1 Kinetic terms

For the fermions, transforming between the higher derivative formalism and the LW picture is slightly more involved. The higher derivative term Eq. (9) generates a Dirac-type mass for the associated LW fields. Therefore each SM fermion, treated as a massless chiral field before electroweak symmetry breaking, receives one left- and one right-handed LW fermion partner. This results in an apparent tripling of the number of degrees of freedom, rather than a doubling as seen in the scalar sector. Alternatively, since they are charged, it is clear that the LW fermions need to have a mass-term of the Dirac-type necessitating left- and right-handed fields of the same $\text{SU}(2)_L$ representation.

2.3.2 Yukawa interactions and physical masses

After introducing the required auxiliary fields and performing a shift in the field variable, as described above, the Yukawa interactions for the quarks take the following form

$$\mathcal{L}_{\text{Yuk}} = g_u^{ij} (\bar{u}_R^i - \bar{\tilde{u}}_R^i) (H - \tilde{H}) \epsilon (Q_L^j - \tilde{Q}_L^j) - g_d^{ij} (\bar{d}_R^i - \bar{\tilde{d}}_R^i) (H^\dagger - \tilde{H}^\dagger) (Q_L^j - \tilde{Q}_L^j) + \text{h.c.} \quad (21)$$

In the lepton sector the Yukawa interactions also take a similar form. All quarks apart from the top quark will be assumed to be massless, which is expected to be a good approximation in the limit that the LW mass scales are larger than the top mass $m_{t,\text{phys}}$. Only one Yukawa coupling will therefore be considered, $g_u^{33} \simeq 1$. It will also be assumed that the LW mass matrices of the \tilde{Q}_L and \tilde{u}_L are diagonal. Such an assumption is compatible with the principle of Minimal Flavour Violation (MFV) [16].

An additional Yukawa term coupling the right-handed $\text{SU}(2)_L$ doublet fermion and the left-handed $\text{SU}(2)_L$ fermion singlet is allowed by the $\text{SU}(2)_L$ symmetry. This could have been written

$$\delta\mathcal{L}_{\text{Yuk}} \sim \overline{\tilde{u}'_L}(Y_H H + Y_{\tilde{H}} \tilde{H})\epsilon Q'_R, \quad (22)$$

but it is not required by the model. As pointed out in appendix A, this term does not have any impact on the results of our paper and it is therefore neglected in the following.

For the diagonalization of the fermion mass matrix it is convenient to put each flavour into a three dimensional vector, such that

$$\Psi_L^{t\top} = (T_L, \tilde{T}_L, \tilde{t}'_L), \quad \Psi_R^{t\top} = (t_R, \tilde{t}_R, \tilde{T}'_R), \quad (23)$$

where T_L is a component of the third generation SM doublet Q_L

$$Q_{L3} = \begin{pmatrix} T_L \\ B_L \end{pmatrix}, \quad (24)$$

Lower case fermions denote $\text{SU}(2)_L$ singlets. Note that each chiral fermion, taking T_L as an example, necessitates two chiral fermion partners, \tilde{T}_L and \tilde{T}'_R , to form the massive LW degree of freedom. In this formalism, the neutral Higgs-top interactions are given by

$$\mathcal{L} = \frac{\sqrt{2}}{v}(h_0 - \tilde{h}_0) \overline{\Psi_R^t} g_t \Psi_L^t + \text{h.c.} \quad (25)$$

Here, the parametrisation of the Higgs fields introduced in Eq. (12) has been employed and the Yukawa couplings are encoded in the matrix

$$g_t = \begin{pmatrix} m_t & -m_t & 0 \\ -m_t & m_t & 0 \\ 0 & 0 & 0 \end{pmatrix}. \quad (26)$$

The presence of two LW fermion partners means the diagonalization of the fermion mass matrices is slightly more involved than the scalar case [3]. The kinetic term assumes the following form

$$\mathcal{L}_{\text{kin}} = \overline{\Psi^t} i \eta_3 \hat{D} \Psi^t - \overline{\Psi_R^t} \mathcal{M}_t \eta_3 \Psi_L^t - \overline{\Psi_L^t} \eta_3 \mathcal{M}_t^\dagger \Psi_R^t, \quad (27)$$

with

$$\mathcal{M}_t \eta_3 = \begin{pmatrix} m_t & -m_t & 0 \\ -m_t & m_t & -M_u \\ 0 & -M_Q & 0 \end{pmatrix} \quad \text{and} \quad \eta_3 = \begin{pmatrix} 1 & 0 & 0 \\ 0 & -1 & 0 \\ 0 & 0 & -1 \end{pmatrix}. \quad (28)$$

Notice that Eq. (28) incorporates the fermion to SM gauge boson, and fermion to LW gauge boson interactions via the covariant derivative \hat{D} , defined in Eq. (14). These interactions are essential for the calculations in section 4.

The mass matrix \mathcal{M}_t can be diagonalized by separate left and right transformations S_L and S_R satisfying

$$S_L \eta_3 S_L^\dagger = \eta_3 \quad \text{and} \quad S_R \eta_3 S_R^\dagger = \eta_3. \quad (29)$$

The fields $\Psi_{L(R)}$ and the matrices \mathcal{M}_t and g_t transform as

$$\Psi_{L(R),\text{phys}} = \eta_3 S_{L(R)}^\dagger \eta_3 \Psi_{L(R)}, \quad \mathcal{M}_{t,\text{phys}} \eta_3 = S_R^\dagger \mathcal{M}_t \eta_3 S_L \quad \text{and} \quad g_{t,\text{phys}} = S_R^\dagger g_t S_L. \quad (30)$$

The $S_{L(R)}$ can be treated as two symplectic rotations and one unitary transformation. Notice that the matrix $g_{t,\text{phys}}$ is not diagonal in general. In the same way as in the Higgs sector the “phys” symbol will be omitted for the fermions for notational brevity but it will be retained on the matrices and the physical masses for clarity.

Performing the matrix diagonalization analytically leads to lengthy expressions. Therefore, explicit results for the physical masses $\mathcal{M}_{t,\text{phys}}$, the transformation matrices $S_{L,R}$ and the Yukawa couplings $g_{t,\text{phys}}$ will be given as a series expansion in $\varepsilon \equiv m_t/M$, where the limit $M_Q = M_u \equiv M$ is explicitly used:

$$\mathcal{M}_{t,\text{phys}} = M \begin{pmatrix} \varepsilon + \varepsilon^3 & 0 & 0 \\ 0 & +1 - \frac{1}{2}\varepsilon - \frac{3}{8}\varepsilon^2 - \frac{1}{2}\varepsilon^3 & 0 \\ 0 & 0 & +1 + \frac{1}{2}\varepsilon - \frac{3}{8}\varepsilon^2 + \frac{1}{2}\varepsilon^3 \end{pmatrix} + \mathcal{O}(M\varepsilon^4), \quad (31)$$

and

$$S_L = \begin{pmatrix} 1 + \frac{1}{2}\varepsilon^2 & \frac{1}{\sqrt{2}}\varepsilon + \frac{5}{4\sqrt{2}}\varepsilon^2 & \frac{i}{\sqrt{2}}\varepsilon - \frac{5i}{4\sqrt{2}}\varepsilon^2 \\ -\varepsilon^2 & -\frac{1}{\sqrt{2}} + \frac{1}{4\sqrt{2}}\varepsilon + \frac{1}{32\sqrt{2}}\varepsilon^2 & \frac{i}{\sqrt{2}} + \frac{i}{4\sqrt{2}}\varepsilon - \frac{i}{32\sqrt{2}}\varepsilon^2 \\ -\varepsilon & -\frac{1}{\sqrt{2}} - \frac{1}{4\sqrt{2}}\varepsilon - \frac{15}{32\sqrt{2}}\varepsilon^2 & -\frac{i}{\sqrt{2}} + \frac{i}{4\sqrt{2}}\varepsilon - \frac{15i}{32\sqrt{2}}\varepsilon^2 \end{pmatrix} + \mathcal{O}(\varepsilon^3)$$

$$S_R = S_L^*. \quad (32)$$

Finally, the Yukawa couplings are proportional to the matrix

$$g_{t,\text{phys}} = M \begin{pmatrix} \varepsilon + 3\varepsilon^3 & \frac{1}{\sqrt{2}}\varepsilon + \frac{3}{4\sqrt{2}}\varepsilon^2 + \frac{87}{32\sqrt{2}}\varepsilon^3 - \frac{i}{\sqrt{2}}\varepsilon + \frac{3i}{4\sqrt{2}}\varepsilon^2 - \frac{87i}{32\sqrt{2}}\varepsilon^3 \\ \frac{1}{\sqrt{2}}\varepsilon + \frac{3}{4\sqrt{2}}\varepsilon^2 + \frac{87}{32\sqrt{2}}\varepsilon^3 & \frac{1}{2}\varepsilon + \frac{3}{4}\varepsilon^2 + \frac{3}{2}\varepsilon^3 & -\frac{i}{2}\varepsilon - \frac{15i}{16}\varepsilon^3 \\ -\frac{i}{\sqrt{2}}\varepsilon + \frac{3i}{4\sqrt{2}}\varepsilon^2 - \frac{87i}{32\sqrt{2}}\varepsilon^3 & -\frac{i}{2}\varepsilon - \frac{15i}{16}\varepsilon^3 & -\frac{1}{2}\varepsilon + \frac{3}{4}\varepsilon^2 - \frac{3}{2}\varepsilon^3 \end{pmatrix}$$

$$+ \mathcal{O}(M\varepsilon^4) \quad (33)$$

It must be stressed here that the diagonalization of the mass terms is possible only if $M > 3\sqrt{3}m_t/2$. The cubic equation for the physical masses of the top quarks is given in appendix C. Also given in appendix C are expressions for the matrices $g_{t,\text{phys}}$ and $\mathcal{M}_{t,\text{phys}}$ in an expansion more closely related to physical masses.

The simple relation between S_R and S_L in Eq. (32) is due to the fact that for $M_Q = M_u$ the matrix $\mathcal{M}_t \eta_3$ is symmetric. This in turn implies that the property $g_t^\top = g_t$ is preserved by the transformation (30) to the physical matrix $g_{t,\text{phys}}$.

Note that the diagonalization of fermions does not affect the coupling to the gauge bosons in Eq. (27) due to the defining property (29).

2.4 Gauge Bosons

2.4.1 One gauge field

The gauge sector is slightly more involved than the fermion and scalar sectors. As a “warm-up” exercise, first a single gauge sector will be discussed. In this discussion it will become apparent that the auxiliary degree of freedom introduced to deal with the higher derivatives is not a gauge field – the new fields have a mass-term from the start and hence they are truly massive spin-1 fields, i.e. Proca fields.

The gauge sector in the higher derivative formulation is defined through the usual gauge kinetic term $-1/2\text{tr}(\hat{F}_{\mu\nu}\hat{F}^{\mu\nu})$ plus the higher derivative kinetic term given in Eq. (10), which generates new types of interaction terms. The higher derivative term can be eliminated by introducing the auxiliary field \tilde{A}_μ [3]

$$\mathcal{L}_{\text{gauge}} = -\frac{1}{2}\text{tr}(\hat{F}_{\mu\nu}\hat{F}^{\mu\nu}) - M_A^2\text{tr}(\tilde{A}_\mu\tilde{A}^\mu) + 2\text{tr}(\hat{F}_{\mu\nu}\hat{D}^\mu\tilde{A}^\nu), \quad (34)$$

where $\hat{D}_\mu\tilde{A}_\nu = \partial_\mu\tilde{A}_\nu - ig[\hat{A}_\mu, \tilde{A}_\nu]$. Clearly, for an Abelian gauge symmetry the commutator of the gauge fields would vanish. As before, the higher-derivative Lagrangian is obtained by eliminating the auxiliary field by its EoM. Moreover the EoM

$$(\hat{D}^\mu\hat{F}_{\mu\nu})^A + M_A^2(\tilde{A}_\nu)^A = 0 \quad (35)$$

explicitly shows that the auxiliary is *not* a gauge field. Under a local gauge transformation $G(x)$ the two fields \hat{A}_μ and \tilde{A}_μ transform as

$$\begin{aligned} \hat{A}_\mu &\rightarrow G(x) \left(\hat{A}_\mu + \frac{i}{g}\partial_\mu \right) G(x)^{-1} \\ \tilde{A}_\mu &\rightarrow G(x)\tilde{A}_\mu G(x)^{-1}. \end{aligned} \quad (36)$$

The kinetic terms are diagonalized by the field shift $\hat{A}_\mu = A_\mu + \tilde{A}_\mu$, where A_μ transforms as \hat{A}_μ (36) under a local gauge transformation. The Lagrangian then assumes the form

$$\begin{aligned} \mathcal{L}_{\text{gauge}} = & -\frac{1}{2}\text{tr}(F_{\mu\nu}F^{\mu\nu}) + \frac{1}{2}\text{tr}\left((D_\mu\tilde{A}_\nu - D_\nu\tilde{A}_\mu)(D^\mu\tilde{A}^\nu - D^\nu\tilde{A}^\mu)\right) \\ & - M_A^2\text{tr}(\tilde{A}_\mu\tilde{A}^\mu) + \text{tr}\left([\tilde{A}_\mu, \tilde{A}_\mu]\left(-igF^{\mu\nu} - \frac{3}{2}g^2[\tilde{A}^\mu, \tilde{A}^\mu] - 4igD^\mu\tilde{A}^\nu\right)\right). \end{aligned} \quad (37)$$

Note that there are no terms linear in either A_μ or \tilde{A}_μ , as demanded by the diagonalization, which is not immediately obvious from the expression above. The propagators for the fields are

$$D_{\mu\nu}(k) = \frac{i}{k^2} \left(g_{\mu\nu} - (1 - \xi) \frac{k_\mu k_\nu}{k^2} \right)$$

$$D_{\mu\nu}(k) = \frac{i}{k^2 - M_A^2} \left(g_{\mu\nu} - \frac{k_\mu k_\nu}{M_A^2} \right). \quad (38)$$

The standard R_ξ gauge has been chosen for the gauge field A_μ . As already emphasized, the field \tilde{A}_μ is not a gauge field, its propagator is that of a massive vector field, formally identical to that of, say, the W gauge boson propagator in unitary gauge. This fact will be further exploited in section 4.2 when calculating the W loop contribution to $h_0 \rightarrow \gamma\gamma$.

2.4.2 The complete SM gauge sector

In this section, the mass diagonalization of the gauge sector in the LWSM will be addressed. After electroweak symmetry breaking, the masses of the electroweak gauge bosons have the following form

$$\mathcal{L}_{\text{gauge}} = \frac{1}{2} \mathcal{B}_\mu^\top \mathcal{M}_\mathcal{B} \eta_4 \mathcal{B}^\mu + \frac{1}{2} \mathcal{W}_\mu^{a\top} \mathcal{M}_\mathcal{W} \eta_2 \mathcal{W}^{a\mu}, \quad \text{where } \eta_4 = \text{diag}(1, 1, -1, -1),$$

$$\mathcal{M}_\mathcal{B} \eta_4 = \begin{pmatrix} M_{\text{SM}} & M_{\text{SM}} \\ M_{\text{SM}} & M_{\text{SM}} - M_{12} \end{pmatrix}, \quad M_{\text{SM}} = \frac{v^2}{4} \begin{pmatrix} g_1^2 & -g_1 g_2 \\ -g_1 g_2 & g_2^2 \end{pmatrix},$$

$$\mathcal{M}_\mathcal{W} \eta_2 = \frac{1}{4} \begin{pmatrix} g_2^2 v^2 & g_2^2 v^2 \\ g_2^2 v^2 & g_2^2 v^2 - 4M_2^2 \end{pmatrix}, \quad M_{12} = \begin{pmatrix} M_1^2 & 0 \\ 0 & M_2^2 \end{pmatrix}. \quad (39)$$

In the equations above, $a = \{1, 2\}$, $\mathcal{B}_\mu^\top = (B_\mu, W_\mu^3, \tilde{B}_\mu, \tilde{W}_\mu^3)$, $\mathcal{W}_\mu^{a\top} = (W_\mu^a, \tilde{W}_\mu^a)$ and M_1, M_2 are the LW masses in the gauge boson sector.

The 2×2 matrix $\mathcal{M}_\mathcal{W} \eta_2$ is diagonalized by a symplectic transformation such that

$$\mathcal{W}_{\text{phys}} = \eta_2 S_W^\dagger \eta_2 \mathcal{W}. \quad (40)$$

The matrix S_W satisfies

$$S_W = \begin{pmatrix} \cosh \psi_W & \sinh \psi_W \\ \sinh \psi_W & \cosh \psi_W \end{pmatrix}, \quad S_W \eta_2 S_W^\dagger = \eta_2, \quad (41)$$

where

$$\tanh 2\psi_W = \frac{g_2^2 v^2}{2M_2^2 - g_2^2 v^2}, \quad (42)$$

and

$$m_{W,\text{phys}}^2 = \frac{1}{2} \left(M_2^2 - \sqrt{M_2^4 - g_2^2 v^2 M_2^2} \right),$$

$$m_{\tilde{W},\text{phys}}^2 = \frac{1}{2} \left(M_2^2 + \sqrt{M_2^4 - g_2^2 v^2 M_2^2} \right). \quad (43)$$

The 4×4 matrix $\mathcal{M}_{\mathcal{B}} \eta_4$ is diagonalized by a combination of symplectic and orthogonal transformations such that mixing between the upper two and lower two components occurs via a symplectic rotation and mixing amongst either the upper or lower two components occurs via an orthogonal rotation. Under this transformation,

$$\mathcal{B}_{\text{phys}} = \eta_4 S_B^\dagger \eta_4 \mathcal{B}, \quad (44)$$

and one physical mass is guaranteed to be zero (corresponding to the photon).

In the following, it will be assumed that mixing between the SM and LW sectors can be treated as a perturbation to the usual SM mixing [3]. This allows the upper 2×2 block of $\mathcal{M}_{\mathcal{B}}$ to be diagonalized by an orthogonal rotation about an angle θ_W , the usual weak mixing angle. The LW fields can then be diagonalized by another orthogonal rotation with a mixing angle

$$\tan 2\phi_W = \frac{g_1 g_2 v^2}{2} \left(M_1^2 - M_2^2 + (g_1^2 - g_2^2) \frac{v^2}{4} \right)^{-1}. \quad (45)$$

Hence, depending on the actual values of M_1 and M_2 this angle can assume any value and for $M_1 = M_2$ it is, not surprisingly, identical with the original Weinberg angle.

As pointed out by GOW [3], mixing between the neutral SM and LW gauge bosons will lead to a tree-level contribution to the electroweak ρ parameter. Bounds on $\Delta\rho$ place constraints on M_1 such that $M_1 \gtrsim 1$ TeV, thus placing bounds on the masses of the neutral LW gauge bosons. Clearly a more careful analysis would be desirable, but for the purposes of this work $M_1 > 1$ TeV will be assumed. It should be pointed out that measurements of muon decay do not set a tree level constraint on the mass of the LW W boson, contrary to models with a W' [17]. This can for instance be seen in the higher derivative formulation by observing that the propagator (2) at zero momentum transfer $\hat{D}(0) = -i/m^2$ does not contain any trace of the LW mass scale! Bounds on the LW W boson are therefore expected to be less stringent than those on the LW Z boson. Bounds from direct searches for W' 's and Z' 's are model dependent, but are typically in the range 780-920 GeV for heavy SM-like gauge bosons [18].

3 Higher derivatives vs LW formulation

In this section the mechanism responsible for cancelling quadratic divergences is outlined in both the higher derivative formalism, as advocated in Ref. [3], and the original LW formulation [2]. Moreover, at the end of this section some comments on the consequences for finite graphs are added.

Introducing higher derivatives improves the convergence of graphs by adding higher powers of momenta in the propagators. This works as long as potential higher derivatives in the interaction terms do not upset this effect. In the LW model higher derivatives are introduced into the kinetic terms but also to the interaction terms, e.g. $\hat{\phi}^\dagger \hat{D}^4 \hat{\phi}$ (8), through the principle of minimal coupling. It is therefore not obvious that the Higgs boson

self-energy contribution due to gauge fields has any improved convergence. It was pointed out in [3], by assuming the Landau gauge, that the potentially dangerous derivatives in the interaction term can be moved to the external legs. This assures improved convergence, which means that the quadratic divergences are absent. The absence of quadratic divergences in the Higgs boson self energy due to the fermions is immediate in the higher derivative formulation, contrary to the case discussed above, since the Yukawa interaction term is not affected by additional derivatives enforced by a minimal coupling.

It is also instructive to investigate the cancellation of quadratic divergences in the Higgs boson self energy due to fermions in the LW formulation. Naively, it is not obvious how this happens, but since the two formulations are equivalent for physical quantities it is clear that cancellations must take place.

After diagonalization of the fermion states there are nine possible graphs per flavour corresponding to all different pairings of propagators of the fermion states $\Psi_{L(R)}^T = (T_{L(R)}, \tilde{T}_{L(R)}, \tilde{t}'_{L(R)})$. The quadratically divergent part is proportional to

$$\Sigma_H|_{\text{div}} \sim \Lambda_{\text{cut-off}}^2 \text{Tr}[\eta_3 g_{t,\text{phys}} \eta_3 g_{t,\text{phys}}^\dagger] = \Lambda_{\text{cut-off}}^2 \sum_{i,j} |(g_{t,\text{phys}})_{ij}|^2 (-1)^{\delta_{i1}} (-1)^{\delta_{j1}}, \quad (46)$$

which is invariant under the orthosymplectic transformation Eq. (30)

$$I_{g_t} = \text{Tr}[\eta_3 g_{t,\text{phys}} \eta_3 g_{t,\text{phys}}^\dagger] = \text{Tr}[\eta_3 g_t \eta_3 g_t^\dagger]. \quad (47)$$

This is easily verified by the use of the property Eq. (29). Note that the invariant properly takes into account the minus signs of the ghosts. Therefore Eq. (26) implies that the invariant $I_{g_t} = |m_t|^2(1 + 1 - 1 - 1) = 0$ vanishes guaranteeing the absence of quadratic divergences. A quicker way to see this, which has already been advocated in reference [3], is to use the fact that the quadratic divergencies are independent of the mass and that therefore the masses can be set to zero² in which case the states are diagonal from the beginning and the absence of quadratic divergencies again follows from Eq. (26) and the ghosts signs.

It was shown above how quadratic divergences cancel, even in the slightly complicated case of the fermion loop. It is worth pointing out that the quadratic divergences may re-enter via the back door through the mass of the virtual LW particle in cases where the diagrams do not decouple in the infinite mass limit, which is the case for the quadratically divergent subprocesses. A simple example is the quartic Higgs boson self interaction for which the corresponding self energy is

$$\Sigma_H \sim \frac{\lambda}{4\pi^2} \left\{ (\Lambda_{\text{cut-off}}^2 + c m_{h_0,\text{phys}}^2 + \dots) - (\Lambda_{\text{cut-off}}^2 + c m_{\tilde{h}_0,\text{phys}}^2 + \dots) \right\}, \quad (48)$$

where the dots stand for logarithmic corrections. The meaning of this intuitive result is that in order to solve the hierarchy problem the LW Higgs mass should not be much higher than the electroweak scale.

² The limit to zero mass is continuous for fermions and scalars used here, whereas for vectors this is not the case and additional subtleties could arise.

Furthermore, as stated in the introduction it was shown in Ref. [4] that in the context of the see-saw mechanism a heavy neutrino can be embedded into the model without destabilizing the Higgs mass. More precisely a correction of the form $\delta m_{h_0}^2 \sim m_{\nu_R}^2$, which is caused in the see-saw extended SM through the loop of the left handed and right handed neutrino, does not appear in the see-saw extension of the LWSM, as long as $m_{\nu_R} \gg m_{\nu_L}$.

After understanding what happens to processes which are divergent in the SM, it is natural to ask what the impact is on processes which are *finite* in the SM. From the above discussion and the explicit form of the propagators (2) it could be anticipated that the higher derivative formulation implies corrections of the form $(\sqrt{s}/M_{LW})^n$ with s the energy of the process and n some positive integer power. In the LW formulation the same result follows from the viewpoint of the Appelquist–Carazzone decoupling theorem [19].

4 The process $gg \rightarrow h_0 \rightarrow \gamma\gamma$ in the Lee-Wick SM

The discussion of the process $gg \rightarrow h_0 \rightarrow \gamma\gamma$ is one of the main topics of this paper since it has a huge importance for Higgs boson searches, especially for comparably low Higgs boson masses. The main Feynman graphs at leading order are depicted in Fig. 1. It is useful to parametrize the ratio of amplitudes in the LWSM to the amplitudes in the SM as

$$\kappa_{gg} = \frac{\mathcal{A}_{\text{LW}}(gg \rightarrow h_0)}{\mathcal{A}_{\text{SM}}(gg \rightarrow h_0)}, \quad \text{and} \quad \kappa_{\gamma\gamma} = \frac{\mathcal{A}_{\text{LW}}(h_0 \rightarrow \gamma\gamma)}{\mathcal{A}_{\text{SM}}(h_0 \rightarrow \gamma\gamma)}. \quad (49)$$

The ratio of the cross-section times decay rate for the full process $gg \rightarrow h_0 \rightarrow \gamma\gamma$ therefore reads

$$\frac{\sigma_{\text{LW}}(gg \rightarrow h_0) \Gamma_{\text{LW}}(h_0 \rightarrow \gamma\gamma)}{\sigma_{\text{SM}}(gg \rightarrow h_0) \Gamma_{\text{SM}}(h_0 \rightarrow \gamma\gamma)} = |\kappa_{gg}|^2 |\kappa_{\gamma\gamma}|^2. \quad (50)$$

Differences between the SM and the LWSM show up in the process $gg \rightarrow h_0 \rightarrow \gamma\gamma$ because of additional degrees of freedom propagating in loops and also because of effects due to the mixing of the SM and LW fields e.g. Eq. (17),

$$\begin{aligned} h_0 &= \cosh \phi_h h_{0,\text{phys}} + \sinh \phi_h \tilde{h}_{0,\text{phys}} \\ \tilde{h}_0 &= \sinh \phi_h h_{0,\text{phys}} + \cosh \phi_h \tilde{h}_{0,\text{phys}}. \end{aligned} \quad (51)$$

The mixing factors, which will be denoted by the letter s , are easily read off from Eq. (16) and (17)³:

$$\begin{aligned} s_H = \cosh \phi_h &= \frac{1}{(1 - r_{h_0}^4)^{1/2}}, \quad r_{h_0} \equiv \frac{m_{h_0,\text{phys}}}{m_{\tilde{h}_0,\text{phys}}}, \\ s_{H-\tilde{H}} = \cosh \phi_h - \sinh \phi_h &= \frac{1 + r_{h_0}^2}{(1 - r_{h_0}^4)^{1/2}}, \end{aligned} \quad (52)$$

³ Note that the symplectic mixing angle ϕ_h is negative.

where the subscripts denote the type of interaction coupling. Yukawa interactions couple the fermions to the combination $H - \tilde{H}$ (c.f. Eq. (21)) and so the correction to this vertex is denoted $s_{H-\tilde{H}}$. As discussed in section 2.2.1, the LW Higgs does not couple to the gauge bosons via a trilinear coupling in the interaction basis, and therefore the Higgs-to-gauge boson vertex is scaled by a factor s_H .

4.1 $gg \rightarrow h_0$

The process $gg \rightarrow h_0$ is mediated by a fermion triangle loop as depicted in Fig. 1(1A). In the SM the top contribution is the only relevant contribution, c.f. appendix B. The graph essentially counts the number of heavy quarks $m_{Q,\text{phys}} \gtrsim m_{t,\text{phys}}$. The fermion loop without couplings scales as $1/m_f$ in the heavy mass limit, obeying the decoupling theorem. The total vertex is independent of the fermion mass since the Yukawa coupling is proportional to m_f . From the discussion in the previous section the crucial question is what the power correction $m_{h_0}/m_{t,\tilde{t},\tilde{t}',\text{phys}}$ is. The analysis will be first outlined in the LW formulation, and then the argument will be given in the higher derivative formulation.

After noticing how the triangle graph scales with the fermion mass, it is clear that the effective vertex in the LW formulation is proportional to

$$\Gamma_{ggh_0} \sim \text{Tr}[g_{t,\text{phys}} \eta_3 \mathcal{M}_{t,\text{phys}}^{-1}] + O(1/\beta_t), \quad (53)$$

where $\beta_t = 4m_{t,\tilde{t},\tilde{t}',\text{phys}}^2/m_{h_0,\text{phys}}^2$ is the threshold parameter. Note that the first term is independent of the actual values of the various top quark masses and the remainder stands for the asymptotic corrections to the $m_t \rightarrow \infty$ limit. The leading term is invariant under the orthosymplectic transformation of Eq. (30). Moreover it has the additional curious property,

$$I_t = \text{Tr}[g_{t,\text{phys}} \eta_3 \mathcal{M}_{t,\text{phys}}^{-1}] = \text{Tr}[g_t \eta_3 \mathcal{M}_t^{-1}] = 1, \quad (54)$$

of being equal to one, which is explicitly demonstrated in appendix A. Furthermore, the invariant remains unity even if a Yukawa term of the form Eq. (22) would be added; again this finding is discussed in more detail in appendix A.

Another way to understand this result is by inspecting the fermion propagator of the higher derivative formulation. The additional term in Eq. (9) leads to a propagator

$$\hat{S}_F(p) = \frac{\not{p}(1 - \frac{p^2}{M^2}) + m}{p^2(1 - \frac{p^2}{M^2})^2 - m^2}. \quad (55)$$

Notice that the graph remains finite because the increase in convergence coming from the fermion propagators is sufficient to compensate for higher-derivative interaction terms of the form $\delta\mathcal{L}_{hd} \sim \tilde{t}(\partial^2/M^2)\mathcal{A}t$. The fermion triangle graph has a SVV structure and the trace over the Dirac matrices vanishes unless the SM fermion mass term m is picked up. This means by power counting that the correction from the LW fermions is of the order of $\mathcal{O}(s/M^2)$ and therefore the power is $n = 2$. The scaling arguments in the SM would in principle allow for $n = 1$. In the higher-derivative formulation this does not happen

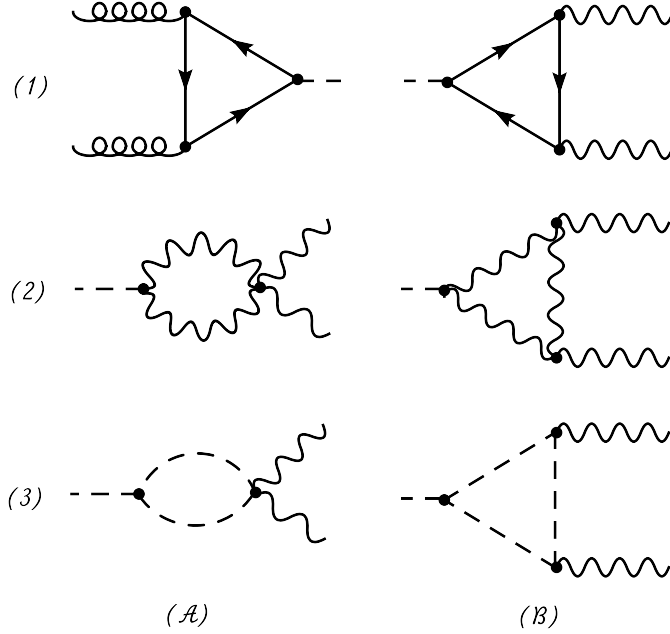


Figure 1: (1A) fermion loop to $gg \rightarrow h_0$. (1B) fermion, (2A, 2B) W boson and (3A, 3B) would-be Goldstone boson (SM) or charged Higgs boson (LW) contribution to $h_0 \rightarrow \gamma\gamma$. In the SM, the dominant contribution to $gg \rightarrow h_0$ stems from the top quark and the dominant contribution to $h_0 \rightarrow \gamma\gamma$ is due to the W^\pm .

because the LW fermion mass M does not enter with a term proportional to the unit matrix, in contrast to the SM fermion mass m . Notice that the difference in the structure of the SM and LW mass terms is transparent in the higher derivative formalism but not in the LW formalism. In the LW formulation the scaling of the pure loops is $1/m_f$, as stated above, but the diagonalization of the Yukawa matrix exactly cancels this effect. Furthermore, this implies that the Yukawa element $(g_{t,\text{phys}})_{11} > m_{t,\text{phys}}$ which is unusual and due to the ghost-like nature of the LW particles. The consequences for the CKM elements $|V_{t(d,s,b)}|$ will be discussed later, in section 5.

Finally, the κ factor for the process $gg \rightarrow h_0$ is then simply given by ⁴

$$\kappa_{gg} = \frac{s_{H-\tilde{H}} \tilde{F}_{1/2}}{F_{1/2}(\beta_t)}, \quad (56)$$

with

$$\tilde{F}_{1/2} = \frac{(g_{t,\text{phys}})_{11}}{m_{t,\text{phys}}} F_{1/2}(\beta_t) - \frac{(g_{t,\text{phys}})_{22}}{m_{\tilde{t},\text{phys}}} F_{1/2}(\beta_{\tilde{t}}) - \frac{(g_{t,\text{phys}})_{33}}{m_{\tilde{t}',\text{phys}}} F_{1/2}(\beta_{\tilde{t}'}), \quad (57)$$

where $s_{H-\tilde{H}}$ takes into account the mixing of the SM and LW Higgs and is given in

⁴The quantity $\tilde{F}_{1/2}$ may be written in terms of a trace as: $\tilde{F}_{1/2} = \text{Tr}[g_{t,\text{phys}} \eta_3 \mathcal{M}_{t,\text{phys}}^{-1} F]$ with $F = \text{diag}[F_{1/2}(\beta_t), F_{1/2}(\beta_{\tilde{t}}), F_{1/2}(\beta_{\tilde{t}'})]$.

Eq. (52). The threshold parameter β_x is

$$\beta_x = \frac{4m_{x,\text{phys}}^2}{m_{h_0,\text{phys}}^2}. \quad (58)$$

The form factor $F_{1/2}$ is given in the appendix B Eq. (A.10).

4.2 $h_0 \rightarrow \gamma\gamma$

In addition to the top quark loop, already discussed for the process $gg \rightarrow h_0$, the process $h_0 \rightarrow \gamma\gamma$ receives further contributions from the W boson loop Fig. 1(2A,2B) and LW charged Higgs bosons Fig. 1(3A,3B).

The dominant contribution to the process $h_0 \rightarrow \gamma\gamma$ comes from charged gauge boson loops, as can be seen in appendix B. The gauge boson sector of the LW model is studied in section 2.4. A central finding there was that the LW gauge boson propagator (38) has a form identical (up to a sign) to the SM gauge boson propagator in the unitary gauge. Furthermore, all relevant vertices are also identical up to signs. Therefore, in the unitary gauge the LW \tilde{W} boson contribution has an identical form to the SM W boson up to some multiplicative factors. Since the amplitude is independent of the choice of gauge this implies that the LW W boson contribution is finite, although in naive power counting it is not finite. This has been checked through an explicit calculation. Moreover, further graphs containing mixed vertices of the type $\partial\tilde{h}^+h^-A$ can be avoided by choosing the unitary gauge for the $SU(2)_L$ gauge field which decouples the would-be Goldstone bosons from the Lee-Wick charged Higgs bosons.

Taking everything together, the total correction factor $\kappa_{\gamma\gamma}$ is thus given by

$$\kappa_{\gamma\gamma} = \frac{s_{H-\tilde{H}} (N_c Q_t^2) \tilde{F}_{1/2} + s_H \tilde{F}_1 + s_{H-\tilde{H}} \tilde{F}_0^\varphi}{(N_c Q_t^2) F_{1/2} + F_1}, \quad (59)$$

where the form factors $F_{1/2}$ and F_1 are given in appendix B and the tilde form factors shall be discussed below. The SM and LW Higgs mixing factors $s_{H-\tilde{H}}$ and s_H are given in Eq. (52). In contrast to the SM, the LW model has an additional contribution from charged LW Higgs bosons running in the loop⁵. Their Feynman rules may be read off from the Lagrangian in Eq. (13) and the parametrisation (12). The top fermion contributions $\tilde{F}_{1/2}$ are the same as in the previous section Eq. (57). As discussed above, the LW \tilde{W} boson contribution is the same as in the SM up to factors which are easily read off from the Lagrangian. There is also an effect due to the mixing of the W bosons Eq. (40)

$$\begin{aligned} W &= \cosh \psi_W W_{\text{phys}} + \sinh \psi_W \tilde{W}_{\text{phys}}, \\ \tilde{W} &= \sinh \psi_W W_{\text{phys}} + \cosh \psi_W \tilde{W}_{\text{phys}}, \end{aligned} \quad (60)$$

⁵ The form of their loop factor, of course, is identical to that of the would-be Goldstone bosons of the SM in non-linear R_ξ gauge.

which results in a correction factor $s_{(A+\tilde{A})^2}$, similar to s_H and $s_{H-\tilde{H}}$ in Eq. (52), for the $h_0 WW$ and $h_0 \tilde{W} \tilde{W}$ vertices

$$s_{(A+\tilde{A})^2} = (\cosh \psi_W + \sinh \psi_W)^2 = \frac{1 + r_W^2}{1 - r_W^2}, \quad r_W \equiv \frac{m_{W,\text{phys}}}{m_{\tilde{W},\text{phys}}}. \quad (61)$$

The full W boson contribution is then given by

$$\tilde{F}_1 = s_{(A+\tilde{A})^2} \rho_{vW} \left[F_1(\beta_W) - \left(\frac{m_{W,\text{phys}}}{m_{\tilde{W},\text{phys}}} \right)^2 F_1(\beta_{\tilde{W}}) \right], \quad (62)$$

where the ρ_{vW} factor will be explained at the end of this section. The correction $s_{(A+\tilde{A})^2}$ to \tilde{F}_1 is analogous to the correction $(g_{t,\text{phys}})_{11}/m_{t,\text{phys}} \dots$ to $\tilde{F}_{1/2}$ in Eq. (57). The combined pairs of vertices ($WWA, \tilde{W}\tilde{W}A$) and ($WWAA, \tilde{W}\tilde{W}AA$), appearing in the diagrams shown in Fig. 1(2A,2B), are left unchanged under the mixing. From a formal point of view this has to be the case since the triangle graph with the first two couplings (Fig. 1(2B)) and the self-energy graphs (Fig. 1(2A)) are not separately gauge invariant. This effect is achieved by the fact that the vertex pairs have opposite signs and substitution of Eq. (60) gives an overall factor of, $\cosh \psi_W^2 - \sinh \psi_W^2 = 1$, unity. Finally the scalar form factor is given by

$$\tilde{F}_0^\varphi = -\rho_{vH} \left(\frac{m_{h_0,\text{phys}}}{m_{\tilde{h}_+,\text{phys}}} \right)^2 \frac{F_0^\eta(\beta_{\tilde{h}_+})}{2}.$$

The factors of $\rho_{vH,vW}$ stand for the mass ratios

$$\begin{aligned} \rho_{vH} &= \frac{(\lambda^2 v^2/2)}{m_{h_0,\text{phys}}^2} = \frac{1}{1 + r_{h_0}^2}, \quad r_{h_0}^2 = \frac{m_{h_0,\text{phys}}^2}{m_{\tilde{h}_+,\text{phys}}^2}, \\ \rho_{vW} &= \frac{(g^2 v^2/4)}{m_{W,\text{phys}}^2} = \frac{1}{1 + r_W^2}, \quad r_W^2 = \frac{m_{W,\text{phys}}^2}{m_{\tilde{W},\text{phys}}^2}, \end{aligned} \quad (63)$$

of Standard Model versus physical Lee-Wick masses of the Higgs and the W boson respectively and can be obtained from Eq. (20) and by inverting Eq. (43). They take care of the fact that the amplitudes decouple as $1/m_{\text{loop}}^2$ i.e. the inverse of the squared mass of the loop particle.

4.3 Quantitative analysis

In Fig. 2 the dimensionless correction factors $s_H(r_{h_0})$, $s_{H-\tilde{H}}(r_{h_0})$, (defined in Eq. (52)) and $s_{(A+\tilde{A})^2}(r_W)$ (defined in Eq. (61)) are plotted as functions of r_{h_0} or r_W , respectively. Notice that as $r \rightarrow 1$ the correction factors increase sharply, corresponding to the case where the LW and SM masses become degenerate. In this limit, interference effects between the LW and SM contributions to a process should be carefully treated. For this

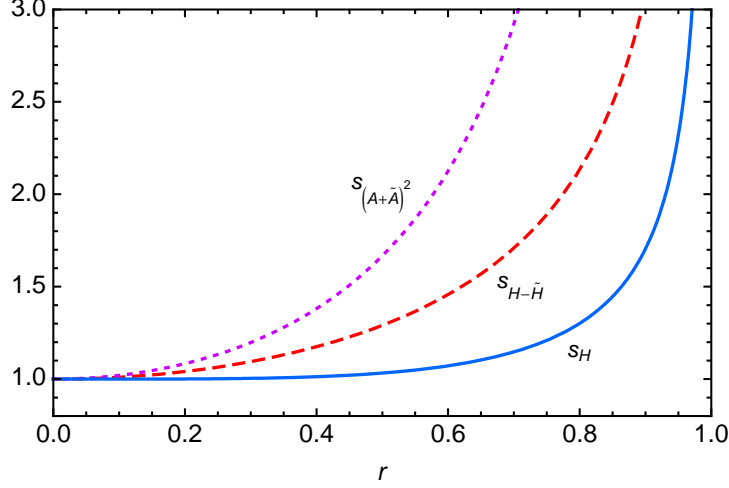


Figure 2: Plots of the dimensionless correction factors, $s_H(r_{h_0})$, $s_{H-\tilde{H}}(r_{h_0})$ (52) and $s_{(A+\tilde{A})^2}(r_W)$ (61) as a function of $r_{h_0} \equiv m_{h_0,\text{phys}}/m_{\tilde{h}_0,\text{phys}}$ and $r_W \equiv m_{W,\text{phys}}/m_{\tilde{W},\text{phys}}$.

work, the masses of the SM and LW Higgs bosons will be assumed to be sufficiently well separated such that only the production and decay of an on-shell SM-like Higgs will need to be considered.

Constraints on the various LW gauge boson mass scales were discussed in Ref. [3] and in section 2.4. In particular, experimental constraints on $\Delta\rho$ placed bounds on the mass M_1 (corresponding to the mass of the LW heavy “photon” in the limit that $M_{(1,2)} \gg g_{(1,2)} v$) such that $M_1 \gtrsim 1$ TeV. However, since there is no tree-level constraint from muon decay on the LW \tilde{W} mass (corresponding to M_2 in the limit $M_{(1,2)} \gg g_{(1,2)} v$) we will assume M_2 could be lower than 1 TeV. Similar assumptions will also be made for the LW top quarks and the LW Higgs bosons such that the analysis can be performed with a common LW scale defined as, $\tilde{M} \equiv M_Q = M_u = m_{\tilde{h}_0,\text{phys}} = m_{\tilde{h}_+,\text{phys}} = m_{\tilde{W},\text{phys}}$.

The upper plot in Fig. 3 shows the relative change in the cross-section, with respect to the SM, for the processes $gg \rightarrow h_0$ in the LWSM. This is displayed as a function of the SM-like Higgs boson mass $m_{h_0,\text{phys}}$. The lower plot in Fig. 3 shows the relative change in the decay rate $h_0 \rightarrow \gamma\gamma$ in the LWSM, also as a function of the SM-like Higgs boson mass $m_{h_0,\text{phys}}$. It is immediately apparent that the effects on the cross-section $gg \rightarrow h_0$ are much larger than those on the rate $h_0 \rightarrow \gamma\gamma$. This can be traced back to the dependence of κ_{gg} on $s_{H-\tilde{H}}$, which rises strongly when the SM Higgs mass $m_{h_0,\text{phys}}$ approaches the LW Higgs mass $m_{\tilde{h}_0,\text{phys}}$.

For Higgs boson masses $m_{h_0,\text{phys}} = 130$ GeV the correction to the rate for $gg \rightarrow h_0$ varies between +4% and +16% for LW masses \tilde{M} between 1000 GeV and 500 GeV, respectively. For Higgs boson masses even closer to the LW scale the corrections can be much larger, cf. Fig. 3.

The corrections to the decay rate $h_0 \rightarrow \gamma\gamma$ are smaller but negative for the same Higgs mass $m_{h_0,\text{phys}} = 130$ GeV. For LW masses \tilde{M} between 1000 GeV and 500 GeV the

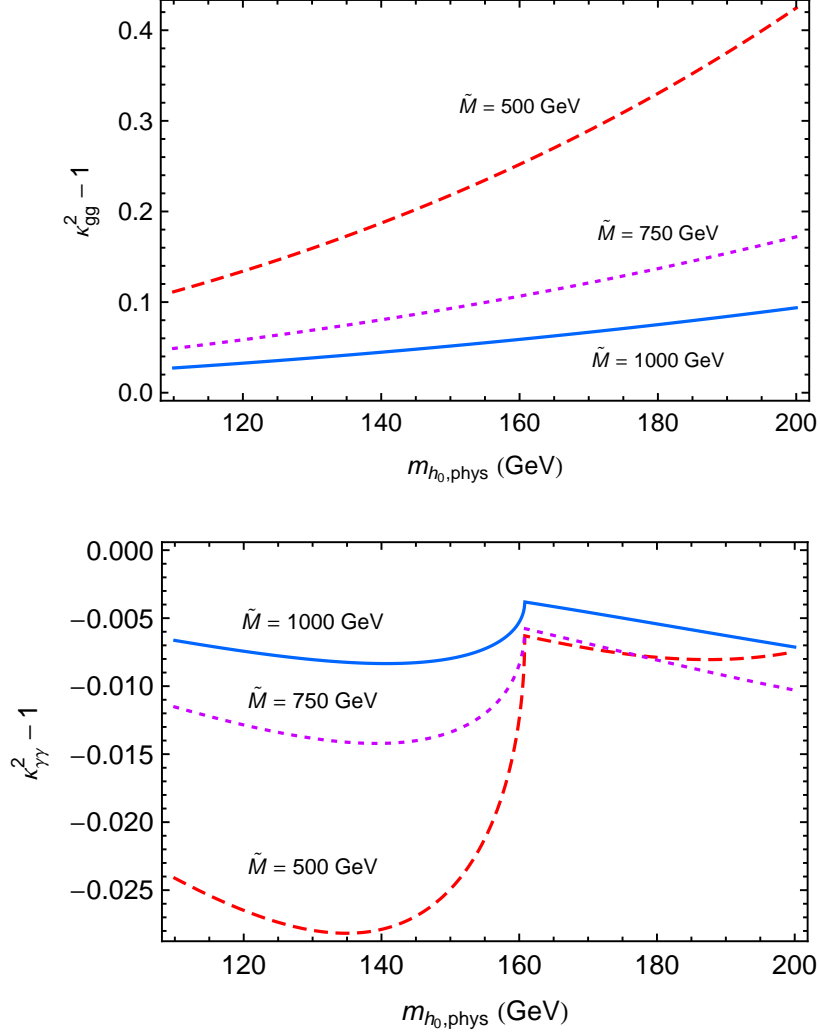


Figure 3: The relative changes in the rates for $gg \rightarrow h_0$ and $h_0 \rightarrow \gamma\gamma$ in the LWSM, expressed as $|\kappa_{gg}|^2 - 1$ and $|\kappa_{\gamma\gamma}|^2 - 1$ respectively, plotted as a function of $m_{h_0, \text{phys}}$. Lee-Wick mass scales are such that $M_Q = M_u = m_{\tilde{h}, \text{phys}} = m_{\tilde{h}^+, \text{phys}} = m_{\tilde{W}, \text{phys}} \equiv \tilde{M}$

corrections are between -0.8% and -2.8% , respectively. Notice that these corrections do not rise strongly for larger Higgs masses (in the range $[110 - 200]$ GeV) because the dominant contribution to the process $h_0 \rightarrow \gamma\gamma$ comes from W -boson loops which have a coupling to the Higgs boson modified by the much more slowly rising s_H correction factor.

Fig. 4 shows the relative change in the cross section times decay rate, $\sigma(gg \rightarrow h_0) \Gamma(h_0 \rightarrow \gamma\gamma)$, Eq. (50). For $m_{h_0, \text{phys}} = 130$ GeV with a LW mass scale $\tilde{M} = 500$ GeV, the enhancement in the rate is $\sim 12\%$. For $m_{h_0, \text{phys}}$ closer to the LW scale the rate is enhanced even more due mainly to the enhancement of $gg \rightarrow h_0$ discussed above.

However, the quantity with direct impact on experimental measurements is more likely to be the total rate

$$\sigma(gg \rightarrow h_0) \text{Br}(h_0 \rightarrow \gamma\gamma). \quad (64)$$

The relative change in this quantity is plotted in Fig. 5. The effects are found to be

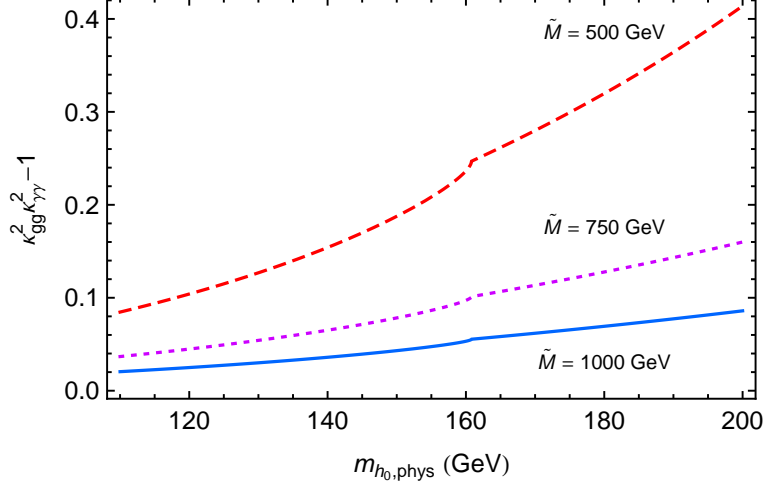


Figure 4: *The relative change in the cross-section times decay rate for the full process $gg \rightarrow h_0 \rightarrow \gamma\gamma$ in the LWSM, expressed as $|\kappa_{gg}|^2 |\kappa_{\gamma\gamma}|^2 - 1$, plotted as a function of $m_{h_0, \text{phys}}$. Lee-Wick mass scales are such that $M_Q = M_u = m_{\tilde{h}, \text{phys}} = m_{\tilde{h}^+, \text{phys}} = m_{\tilde{W}, \text{phys}} \equiv \tilde{M}$*

smaller than the changes in the cross section times decay rate because of the simultaneous enhancement of the total Higgs width in the LWSM. This enhancement almost cancels the effects of the larger cross section times decay rate for lighter Higgs masses and is responsible for the overall small reduction in the total rate for Higgs masses up to about 135 GeV.

The Higgs width in the SM $\Gamma(h_0 \rightarrow \text{all})$ is well approximated by

$$\Gamma(h_0 \rightarrow \text{all}) = \Gamma(h_0 \rightarrow (\bar{f}f, ZZ, W^+W^-)), \quad (65)$$

where $\bar{f}f$ can be $\bar{b}b$, $\bar{\tau}\tau$ or $\bar{c}c \dots$ and potentially off-shell gauge bosons are also included. The total Higgs boson width in the LWSM can be obtained by scaling the individual SM decay rates (for the tree level processes). Using Eqs. (52) and (61), the vector boson modes are scaled by a factor $s_H^2 s_{(A+\tilde{A})}^2$ and the $\bar{f}f$ modes are scaled by a factor $s_{H-\tilde{H}}^2$.

A technique for measuring the Higgs boson couplings $g g h_0$ and $\gamma \gamma h_0$ at the LHC was discussed in Ref. [20]. With $2 \times 300 \text{ fb}^{-1}$ of integrated luminosity, it was estimated that a new contribution to the $g g h_0$ coupling could be measured if the corresponding partial width was larger than $\pm(30 - 45)\%$ of the SM expected value, for Higgs boson masses in the range $110 \lesssim m_{h_0, \text{phys}} \lesssim 190 \text{ GeV}$. The prospects for measuring a new contribution to the $\gamma \gamma h_0$ coupling are slightly better. If a new contribution to the partial width for $h_0 \rightarrow \gamma \gamma$ is larger than $\pm(15 - 20)\%$ of the SM expected value, then it should be measurable for Higgs masses in the range $120 \lesssim m_{h_0, \text{phys}} \lesssim 140 \text{ GeV}$.

Notice from Fig. 3 that the expected changes in the $h_0 \rightarrow g g$ and $h_0 \rightarrow \gamma \gamma$ partial widths in the LWSM fall just short of the expected reach of the LHC with $2 \times 300 \text{ fb}^{-1}$ of integrated luminosity. It could be hoped that more luminosity would uncover these small deviations, however, the apparent absence of a deviation from the SM in these channels, combined with the presence of one or more heavy LW resonances (such as a \tilde{W} [12]) could

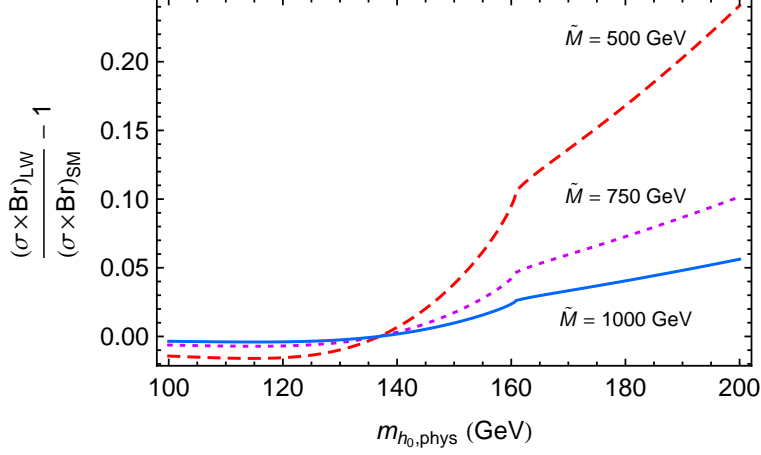


Figure 5: *The relative effect on the experimentally measurable quantity of cross section times branching ratio $\sigma(gg \rightarrow h_0) \text{Br}(h_0 \rightarrow \gamma\gamma)$ in the LWSM, plotted against $m_{h_0,\text{phys}}$ for different values of the LW scale \tilde{M} .*

be taken as evidence for the LWSM. A further potential signature of the LWSM will be discussed in the next section.

5 Enhancement of the CKM elements $|V_{t(d,s,b)}|$

As has already been discussed in Sec. 2.3.2, each of the SM fermions experiences a mixing with the corresponding two chiral LW fermions, proportional to the ratio

$$\varepsilon_{\text{ph}} = m_{f,\text{phys}}/M. \quad (66)$$

While this mixing is negligible for most fermions, it may have an important effect on the top quarks and their LW counterparts, which will affect typical flavour physics observables sensitive to new physics such as $B \rightarrow X_{d,s}\gamma$ or $B_{d,s}$ -mixing.

To see how this works out, consider the interaction of the top quarks and counterparts in the down-type sector, mediated by W bosons. The interaction term in the Lagrangian has the form

$$\begin{aligned} \mathcal{L}_{dWt} &= \sum_{i=d,s,b} [V_{it}^* \bar{\Psi}_L^i \mathcal{W} \Psi_L^t + \text{h.c.}] \\ &= \sum_{i=d,s,b} \left[V_{it}^* \left(\bar{D}_L^i, \bar{\tilde{D}}_L^i, \bar{\tilde{d}}_L^i \right) \mathcal{W} \begin{pmatrix} 1 + \frac{1}{2}\varepsilon_{\text{ph}}^2 & \cdots & \cdots \\ \vdots & \ddots & \vdots \\ \vdots & \cdots & \cdots \end{pmatrix} \begin{pmatrix} T_L \\ \tilde{T}_L \\ \tilde{t}_L \end{pmatrix} + \text{h.c.} \right]. \end{aligned} \quad (67)$$

This implies that the charged current interactions of any down-type quark with the top quark, i.e. any interaction of the form $V_{it}^* \bar{d}_L^i \mathcal{W} t_L$, in LWSM is enhanced by the same amount $1 + \varepsilon_{\text{ph}}^2/2$ w.r.t. the original SM value. Clearly the CKM matrix is then not by

itself unitary anymore. Unitarity, which is tightly connected with the GIM mechanism and renormalizability, is obtained when both LW states and the SM particles are properly accounted for.

Clearly, for the non-top CKM matrix elements, which are obtained from direct measurements, LW mixing effects are negligible due to the small SM quark masses.

Up to now, the values of $|V_{td}|$ and $|V_{ts}|$ have only been measured in rare processes, with the top quark running in loops. Therefore, so far, these CKM matrix elements have mainly been measured in products with $|V_{tb}|$, and values for $|V_{td}|$ and $|V_{ts}|$ have been obtained by assuming $|V_{tb}| = 1$ on the grounds of the unitarity of the CKM matrix. Also, many of those measurements in fact provide values for $|V_{td}/V_{ts}|$, where this extra factor due to the diagonalization in the top sector of the LWSM cancels out exactly.

It is worth noting here that overshooting unitarity is a clear indication of the ghost-like nature of the additional degrees of freedom. In other models including extra positive-norm particles, such as models with four or more quark generations and vector-like quarks, unitarity would be undershot, c.f. Ref. [21] for example.

An additional point should be stressed here, which was already hinted at when commenting on the unitarity of the model above. The rescaling $1 + \varepsilon_{\text{ph}}^2/2$ will of course receive corrections from the propagation of intermediate LW partners. This will lead to a decrease in the effect. Such mutual cancellations of mixing and additional particles will probably render constraints on the LWSM from flavour physics less stringent than naively expected from either the negative contribution of the additional particles or the LW mixing factors alone.

The situation is different for the measurement of $|V_{tb}| = 1.3(2)$ by the DØ collaboration at the Tevatron [22]. The experimental set-up makes sure that the intermediate vector boson has the mass of the SM W boson and is not an exotic heavy degree of freedom. Therefore there will be no decreasing correction to the scaling factor $1 + \varepsilon_{\text{ph}}^2/2$.

An overview of constraints on $|V_{tb}|$ and the implication of new physics models can be found in Ref. [21].

6 Consequences for collider searches

The LWSM would manifest itself through a plethora of resonance-like structures. It should be stressed again that these resonances are effective degrees of freedom of a more fundamental theory rather than true particles, as indicated through their ghost-like nature.

Concerning the Higgs boson spectrum, the LWSM provides a second Higgs doublet with four additional scalars, like many other models beyond the Standard Model, consisting of one heavy CP-even and one CP-odd state plus two charged ones. The latter three are, at tree-level, degenerate in mass, the CP-even state is lifted away from the other objects through mixing with the light SM Higgs boson.

The trilinear vertex of the LW Higgs boson with gauge bosons is enabled through mixing with the SM boson only. The relevant mixing factor is $(s_H - s_{H-\tilde{H}})$, with s_H and $s_{H-\tilde{H}}$ defined in Eq. (52). In other words, the gaugophobic nature of the LW Higgs boson

depends on the level of degeneracy of the two neutral CP-even Higgs bosons. So, as a rough estimate, the Higgs sector of the LWSM looks like the Higgs sector of the MSSM close to the decoupling limit. Hence, in most cases, the heavy Higgs bosons could be found only through their decay into the fermions.

Signatures of additional twelve LW quarks could be found in future colliders. If in addition $M_Q = M_u$ or $M_Q = M_d$, as we have assumed for the top sector, then the LW fermions would be pairwise mass degenerate. This degeneracy in fact is only lifted in the top quark sector, through the non-vanishing SM top quark mass. A similar phenomenon would occur for the LW leptons and neutrinos, but mixing effects would definitely not play a role.

So, at first sight, the situation would look quite similar to the case of the first level of fermions in models with universal extra dimensions (UEDs) [23]. A more careful discussion of this issue, however, is clearly beyond the scope of the present paper and should be the subject of forthcoming studies.

In addition to that, the LWSM gives rise to resonances of all gauge bosons, which could be searched for through standard methods employed in the search of Z' , W' and g' states. This has already been discussed in [12]⁶. Finding them would make the similarity to UED models more manifest, the absence of neutralinos, charginos and gluinos and a mismatch of numbers of states in turn would help ruling out the MSSM or similar supersymmetric models. Of course, again, this statement is to be taken with the caveat of the particles being kinematically accessible.

In contrast to the two other models mentioned in this section, the LWSM has a number of distinguishing features:

- First of all, while both the MSSM and the UED models provide a parity (R -parity or KK -parity), forcing the existence of a lightest, stable supersymmetric or KK partner particle, all LW partners may decay, such that ultimately only SM-like particles emerge. Hence, typically there won't be any signatures - apart from those involving neutrinos in the decay chains - involving large missing E_T fractions.
- Secondly, all LW partners have exactly the same spin as their SM counterparts. A careful measurement of the spins of decaying resonance-like structures through momentum correlations in their decay chains in the spirit, e.g., of [24] will therefore help ruling out the MSSM.
- In order to distinguish the LW model from models like the UED model, a careful analysis of the mass spectrum or the particle mixings may help. The truly unique feature of the model is that the ghost nature of the LW states leads to cancellations whereas the orthosymplectic diagonalization gives rise to an enhancement which results in small effects despite the many resonances, as in the amplitude $gg \rightarrow h_0 \rightarrow$

⁶ There, however, the relative phase of the LW partners of the gauge bosons, which is fixed in the LWSM, has been left open.

$\gamma\gamma$. The UED model [25] is distinct in that the additional KK states lead to purely additional effects.

7 Conclusions

In this paper the process $gg \rightarrow h_0 \rightarrow \gamma\gamma$ was investigated in the LWSM, an extension of the SM proposed by Grinstein, O’Connell and Wise, based on an idea of Lee and Wick. All relevant sectors of the model were diagonalized by orthosymplectic transformations, differing from the usual unitary diagonalization procedure. This difference was necessitated by the ghost-like nature of the LW partners to the SM fields.

Numerically, the changes to the measurable overall cross-section times branching ratio $\sigma(gg \rightarrow h_0) \text{Br}(h_0 \rightarrow \gamma\gamma)$ are rather small, due to compensating effects between the mixing-enhanced couplings and cancellations due to the ghost-like nature of the LW partners running in loops. It has been demonstrated how this effect can be understood from the higher derivative formulation of the theory. In channels other than $h_0 \rightarrow \gamma\gamma$ the larger enhancement of the cross-section $\sigma(gg \rightarrow h_0)$ may be measurable.

Signals of heavy LW resonances at future colliders, taken in combination with the absence of a significant change in $\sigma(gg \rightarrow h_0) \text{Br}(h_0 \rightarrow \gamma\gamma)$ is a distinctive feature of the LWSM.

Further signatures of the LWSM may be found in the top sector, where it has been shown that measurements of $|V_{t(b,s,d)}|$ would show an enhancement from the expected value, contrary to the predictions of, for example, 4th generation models. This enhancement is entirely due to the ghost-like nature of the LW-particles and constitutes another particularly distinctive signature.

Besides experimental constraints on the LW gauge bosons, coming from measurements of $\Delta\rho$, it would certainly be desirable to work out in more detail constraints on the LW top, W’s and Higgs bosons.

Addendum This version is equivalent to the PRD version including the erratum. The corrections in Eq. (59) do not change the conclusions of the arXiv v2 of this paper. It is worth noting that among the three standard electroweak reference parameters α , G_F and m_Z , only m_Z receives corrections at tree level [31]. This has been consistently used throughout this work and earlier versions. It is in this respect that we disagree with the relevant results in [29, 30]. It seems to us that in the arXiv version [29] the corrections to α and G_F have not been taken into account in the range of models considered⁷. Ironically, since the Lee-Wick model has no corrections to those parameters at tree level we do agree with the results in [29] when expanding our results to leading order in one over the Lee-Wick masses squared. However, we do not agree with the JHEP version of the paper [30] where corrections to the Higgs VEV, or equivalently G_F , have been attempted. More precisely we agree with (3.43) in [29] but not with (3.43) in [30].

⁷We cannot make any statement of whether they are small or not in any other models than the LWSM.

Acknowledgments

The authors are grateful to Oliver Brein, Stefan Förste, Nigel Glover, Michael Schmidt and Georg Weiglein for discussions. We are also grateful to Jose Zurita and Giacomo Cacciapaglia for discussion concerning their work. In particular, Terrance Figy was of great help during the beginning stages of this project and provided some insight into the mixing of the LW counterparts of the electroweak gauge bosons. FK thanks the Galileo Galilei Institute for Theoretical Physics for the hospitality and the INFN for partial support during the completion of this work. FK wishes to thank the Marie Curie research training network MCNET (contract number MRTN-CT-2006-035606) for financial support. RZ is supported in part by the Marie Curie research training networks contract Nos. MRTN-CT-2006-035482, FLAVIANET, and MRTN-CT-2006-035505, HEPTOOLS.

A Trace property of the orthosymplectic invariant I_t

In this appendix the unity of the orthosymplectic invariant $I_t = \text{Tr}[g_t \eta_3 \mathcal{M}_t^{-1}]$, as stated in Eq. (54), will be proven. It is instructive to use a slightly more general form of the matrices g_t Eq. (30) and $\mathcal{M}_t \eta_3$ Eq. (28) which will be denoted by a bar. Also, the subscript t for the top will be omitted.

$$\overline{\mathcal{M}} = \begin{pmatrix} A_{11} & A_{12} & 0 \\ A_{21} & A_{22} & -M_u \\ 0 & -M_Q & Y \end{pmatrix} \quad \bar{g} = \begin{pmatrix} A_{11} & A_{12} & 0 \\ A_{21} & A_{22} & 0 \\ 0 & 0 & Y \end{pmatrix}. \quad (\text{A.1})$$

Here, a general 2×2 matrix A has been allowed in the first two indices and the additional Yukawa type interaction Eq. (22).

Now, the question is under which conditions the modified invariant,

$$\bar{I} = \text{Tr}[\bar{g} \eta_3 \overline{\mathcal{M}}^{-1}] = 1, \quad (\text{A.2})$$

remains unity. To answer this, the matrix $\overline{\mathcal{M}}$ is rewritten as

$$\overline{\mathcal{M}} \eta_3 = \bar{g} - M_{Qu} \quad M_{Qu} \equiv \begin{pmatrix} 0 & 0 & 0 \\ 0 & 0 & M_u \\ 0 & M_Q & 0 \end{pmatrix}. \quad (\text{A.3})$$

By writing

$$3 = \text{Tr}[(\bar{g} - M_{Qu})(\bar{g} - M_{Qu})^{-1}] = \bar{I} - \text{Tr}[(M_{Qu})(\bar{g} - M_{Qu})^{-1}] \quad (\text{A.4})$$

the task then reduces to find the conditions for the last term on the right hand side to be -2 . The latter is easily evaluated

$$\text{Tr}[M_{Qu} \eta_3 \overline{\mathcal{M}}^{-1}] = 2A_{11} M_Q M_u \det(\overline{\mathcal{M}} \eta_3)^{-1}, \quad (\text{A.5})$$

observing that only two entries of the \mathcal{M}^{-1} enter the trace. The determinant is

$$\det(\overline{\mathcal{M}}\eta_3) = -A_{11}M_Q M_u + Y\det_2(A) \quad (\text{A.6})$$

and therefore Eq. (A.2) is fulfilled if and only if the determinant of the 2×2 matrix A is zero. This is the case for the matrix \mathcal{M}_t Eq. (28) even when an extra Yukawa term of the type Eq. (22) is considered.

B Triangle graph function

In this appendix the well known results for the triangle graphs for the subprocesses $h_0 \rightarrow gg(\gamma\gamma)$ as shown in Fig. 1, will be given. All results will be parametrised in terms of an effective Lagrangian

$$\mathcal{L}^{\text{eff}} = \frac{-g_2}{16\pi m_{W,\text{phys}}} h_0 \left\{ \begin{array}{c} \frac{1}{2}\alpha_s G^2 F_{gg} \\ \alpha F^2 F_{\gamma\gamma} \end{array} \right\}. \quad (\text{A.7})$$

A term $1/2$ has been factored out in front of the gluon field field strength tensor $G^2 \equiv G_{\mu\nu}^a G^{\mu\nu a}$, which originates from the normalisation of the Gell-Mann matrices $\text{Tr}[\frac{\lambda^a}{2} \frac{\lambda^b}{2}] = \frac{1}{2}\delta^{ab}$. The gluon only couples to the quarks whereas the photon also couples to W -bosons. The number of graphs contributing to the latter can be considerably simplified by employing the background field gauge [26] or a non-linear R_ξ gauge [27] by choosing the gauge parameter such that Higgs-gauge terms and gauge fixing terms cancel. The gluon and photon form factors are parametrised as follows

$$F_{gg} = F_{1/2} \quad F_{\gamma\gamma} = F_{1/2} + F_1, \quad (\text{A.8})$$

Ghosts and unphysical charged scalars contributions have to be added to the W boson contribution

$$F_1 = F_1^W + F_0^\eta + F_0^\varphi, \quad (\text{A.9})$$

where η denotes the ghosts and φ the would-be Goldstone bosons. However, employing the non-linear R_ξ gauge [27] the individual terms read

$$\begin{aligned} F_{1/2} &= -2\beta_f[1 + (1 - \beta_f)f(\beta_f)] \\ F_1^W &= 4\beta_W[1 + (2 - \beta_W)f(\beta_W)] \\ F_0^\eta &= -\beta_W[1 - \beta_W f(\beta_W)] \\ F_0^\varphi &= -\frac{2}{\beta_W} F_0^\eta \end{aligned} \quad (\text{A.10})$$

with threshold parameters $\beta_x = 4m_{x,\text{phys}}^2/m_{H,\text{phys}}^2$ and

$$f(x) = \begin{cases} \text{Arcsin}^2(1/\sqrt{x}) & x \geq 1 \\ -\frac{1}{4}(\ln\left(\frac{1+\sqrt{1-x}}{1-\sqrt{1-x}}\right) - i\pi)^2 & x < 1 \end{cases}. \quad (\text{A.11})$$

The result for $F_{1/2}$ can for instance be found in reference [26]. For the fermion loops it is only the top quark that matters, the size of the b quark loop is below one percent as compared to the top contribution. The sum of the three contributions of the vector

$$F_1 = F_1^W + F_0^\eta + F_0^\varphi = 3\beta_W(2 - \beta_W)f(\beta_W) + 3\beta_W + 2 \quad (\text{A.12})$$

reproduces the result in reference [26].

In the table below values for the form factors are quoted, which are of relevance for the analysis in this publication, namely the asymptotic values for an infinitely heavy loop particle $\beta \rightarrow \infty$, which were first obtained in [28] and shown to be the photonic β -function coefficients [26], and the values for physical threshold parameters for a Higgs mass $m_{h_0, \text{phys}} = 120 \text{ GeV}$.

	$F_{1/2}$	F_1	F_1^W	F_0^η	F_0^φ	
$\beta \rightarrow \infty$	$-\frac{4}{3}$	7	$\frac{20}{3}$	$\frac{1}{3}$	0	(A.13)
$\beta_{\text{phys}} \sim$	-1.37	8.2	8.3	0.5	-0.6	

C Top quark masses and Yukawa couplings

The 3 physical top quark masses squared, $m_{t, \text{phys}}^2$, $m_{\tilde{t}, \text{phys}}^2$ and $m_{\tilde{T}, \text{phys}}^2$ can be conveniently be expressed as the 3 roots of the following cubic polynomial

$$x^3 - (M_Q^2 + M_u^2) x^2 + M_Q^2 M_u^2 x - m_t^2 M_Q^2 M_u^2 = 0. \quad (\text{A.14})$$

Most conveniently for phenomenological analyses the top quark Yukawa couplings $g_{t, \text{phys}}$ and the physical top quark masses $\mathcal{M}_{t, \text{phys}}$ can be expressed in terms of the physical (SM) top quark mass $m_{t, \text{phys}}$, where $\varepsilon_{\text{ph}} = m_{t, \text{phys}}/M$ and $M_Q = M_u \equiv M$,

$$\frac{g_{t, \text{phys}}}{M} = \begin{pmatrix} \varepsilon_{\text{ph}} + 2\varepsilon_{\text{ph}}^3 & \frac{1}{\sqrt{2}}\varepsilon_{\text{ph}} + \frac{3}{4\sqrt{2}}\varepsilon_{\text{ph}}^2 + \frac{55}{32\sqrt{2}}\varepsilon_{\text{ph}}^3 & -\frac{i}{\sqrt{2}}\varepsilon_{\text{ph}} + \frac{3i}{4\sqrt{2}}\varepsilon_{\text{ph}}^2 - \frac{55i}{32\sqrt{2}}\varepsilon_{\text{ph}}^3 \\ \frac{1}{\sqrt{2}}\varepsilon_{\text{ph}} + \frac{3}{4\sqrt{2}}\varepsilon_{\text{ph}}^2 + \frac{55}{32\sqrt{2}}\varepsilon_{\text{ph}}^3 & \frac{1}{2}\varepsilon_{\text{ph}} + \frac{3}{4}\varepsilon_{\text{ph}}^2 + \varepsilon_{\text{ph}}^3 & -\frac{i}{2}\varepsilon_{\text{ph}} - \frac{7i}{16}\varepsilon_{\text{ph}}^3 \\ -\frac{i}{\sqrt{2}}\varepsilon_{\text{ph}} + \frac{3i}{4\sqrt{2}}\varepsilon_{\text{ph}}^2 - \frac{55i}{32\sqrt{2}}\varepsilon_{\text{ph}}^3 & -\frac{i}{2}\varepsilon_{\text{ph}} - \frac{7i}{16}\varepsilon_{\text{ph}}^3 & -\frac{1}{2}\varepsilon_{\text{ph}} + \frac{3}{4}\varepsilon_{\text{ph}}^2 - \varepsilon_{\text{ph}}^3 \end{pmatrix} + \mathcal{O}(\varepsilon_{\text{ph}}^4), \quad (\text{A.15})$$

and

$$\frac{\mathcal{M}_{t, \text{phys}} \eta_3}{M} = \begin{pmatrix} \varepsilon_{\text{ph}} & 0 & 0 \\ 0 & -1 + \frac{1}{2}\varepsilon_{\text{ph}} + \frac{3}{8}\varepsilon_{\text{ph}}^2 & 0 \\ 0 & 0 & -1 - \frac{1}{2}\varepsilon_{\text{ph}} + \frac{3}{8}\varepsilon_{\text{ph}}^2 \end{pmatrix} + \mathcal{O}(\varepsilon_{\text{ph}}^4). \quad (\text{A.16})$$

References

- [1] T. D. Lee and G. C. Wick, Nucl. Phys. B **9** (1969) 209.
- [2] T. D. Lee and G. C. Wick, Phys. Rev. D **2** (1970) 1033.

- [3] B. Grinstein, D. O’Connell and M. B. Wise, arXiv:0704.1845 [hep-ph].
- [4] J. R. Espinosa, B. Grinstein, D. O’Connell and M. B. Wise, arXiv:0705.1188 [hep-ph].
- [5] T. D. Lee, in *Proceedings of the International School of Physics "Ettore Majorana," Erice, Italy, 1970, edited by A. Zichichi, New York, 1971, 63-93*
- [6] S. Coleman, in **Erice 1969, Ettore Majorana School On Subnuclear Phenomena*, New York 1970, 282-327*
- [7] R. E. Cutkosky, P. V. Landshoff, D. I. Olive and J. C. Polkinghorne, Nucl. Phys. B **12** (1969) 281.
- [8] D. G. Boulware and D. J. Gross, Nucl. Phys. B **233** (1984) 1.
- [9] K. Jansen, J. Kuti and C. Liu, Phys. Lett. B **309** (1993) 119 [arXiv:hep-lat/9305003].
- [10] K. Jansen, J. Kuti and C. Liu, Phys. Lett. B **309** (1993) 127 [arXiv:hep-lat/9305004].
- [11] A. van Tonder, Int. J. Mod. Phys. A **22** (2007) 2563 [arXiv:hep-th/0610185].
- [12] T. G. Rizzo, JHEP **0706** (2007) 070 [arXiv:0704.3458 [hep-ph]].
- [13] T. R. Dulaney and M. B. Wise, arXiv:0708.0567 [hep-ph].
- [14] I. Antoniadis, E. Dudas and D. M. Ghilencea, arXiv:0708.0383 [hep-th].
- [15] D. M. Ghilencea, arXiv:0708.2501 [hep-ph].
- [16] G. D’Ambrosio, G. F. Giudice, G. Isidori and A. Strumia, Nucl. Phys. B **645** (2002) 155 [arXiv:hep-ph/0207036].
- [17] W. M. Yao *et al.* [Particle Data Group], J. Phys. G **33** (2006) 1.
- [18] See for example, T. Aaltonen *et al.* [CDF Collaboration], arXiv:0707.2524 [hep-ex].
- [19] T. Appelquist and J. Carazzone, Phys. Rev. D **11** (1975) 2856.
- [20] M. Duhrssen, S. Heinemeyer, H. Logan, D. Rainwater, G. Weiglein and D. Zeppenfeld, Phys. Rev. D **70** (2004) 113009 [arXiv:hep-ph/0406323].
- [21] J. Alwall *et al.*, Eur. Phys. J. C **49** (2007) 791 [arXiv:hep-ph/0607115].
- [22] V. M. Abazov *et al.* [D0 Collaboration], measurement Phys. Rev. Lett. **98** (2007) 181802 [arXiv:hep-ex/0612052].
- [23] T. Appelquist, H. C. Cheng and B. A. Dobrescu, Phys. Rev. D **64** (2001) 035002 [arXiv:hep-ph/0012100].
- [24] A. J. Barr, Phys. Lett. B **596** (2004) 205 [arXiv:hep-ph/0405052].

- [25] F. J. Petriello, JHEP **0205** (2002) 003 [arXiv:hep-ph/0204067].
- [26] M. A. Shifman, A. I. Vainshtein, M. B. Voloshin and V. I. Zakharov, Sov. J. Nucl. Phys. **30** (1979) 711 [Yad. Fiz. **30** (1979) 1368].
- [27] M. B. Gavela, G. Girardi, C. Malleville and P. Sorba, Nucl. Phys. B **193** (1981) 257.
- [28] J. R. Ellis, M. K. Gaillard and D. V. Nanopoulos, Nucl. Phys. B **106** (1976) 292.
- [29] G. Cacciapaglia, A. Deandrea and J. Llodra-Perez, [arXiv:0901.0927v2 [hep-ph]].
- [30] G. Cacciapaglia, A. Deandrea and J. Llodra-Perez, JHEP **0906** (2009) 054
- [31] T. E. J. Underwood and R. Zwicky, “Electroweak Precision Data and the Lee-Wick Standard Model,” Phys. Rev. D **79** (2009) 035016 [arXiv:0805.3296 [hep-ph]].